OPEN ACCESS
IOP Publishing
Journal of Physics A: Mathematical and Theoretical
J. Phys. A: Math. Theor. **58** (2025) 365301 (18pp)
https://doi.org/10.1088/1751-8121/adffcd

Prediction of the relaxation time of a transmon qubit with the steepest-entropy-ascent quantum thermodynamics framework

Luis Enrique Rocha-Soto[1], **Cesar Eduardo Damian-Ascencio**[1], **Adriana Saldaña-Robles**[2] **and Sergio Cano-Andrade**[1,*]

[1] Department of Mechanical Engineering, Universidad de Guanajuato, Salamanca Gto. 36885, Mexico
[2] Department of Agricultural Engineering, Universidad de Guanajuato, Irapuato Gto. 36500, Mexico

E-mail: sergio.cano@ugto.mx

Received 8 April 2025; revised 17 August 2025
Accepted for publication 27 August 2025
Published 5 September 2025

Abstract

Decoherence has been observed to be one of the main limitations to build a practical quantum computer. This is because the qubits that conform it rapidly lose the entanglement and correlations existent among them due to interactions with the environment. In this work, the relaxation time of a Transmon qubit interacting with an environment is predicted by using the steepest-entropy-ascent quantum thermodynamics framework and the Lindblad master equation. For the study it is considered that the environment behaves as a thermal bath composed of a collection of harmonic oscillators. Results show that the qubit processes from a non-equilibrium state to a state of stable equilibrium, exchanging energy with the thermal bath during the process. In addition, the prediction of the relaxation time of the qubit is in agreement with experimental results

* Author to whom any correspondence should be addressed.

obtained from the literature. The decoherence time is also accurately predicted by the models.

Keywords: steepest-entropy-ascent, Lindblad master equation, transmon qubit, relaxation time

1. Introduction

Quantum computing has been growing in recent years, largely driven by the performance of superconducting qubits. These qubits offer key advantages such as high reproducibility, controllability, and scalability, making them a promising platform for large-scale quantum computation [1–3]. However, their inevitable interaction with the surrounding environment induces quantum decoherence, leading to the gradual loss of quantum information [4–6]. This decoherence process poses a significant challenge to maintaining the integrity of quantum states, thereby affecting the performance and reliability of quantum computations [7–9].

Quantum decoherence is typically studied using open quantum system models based on the Born–Markov approximation, which assumes that the system of interest is weakly coupled to and interacts with an environment or thermal bath. According to Gemmer *et al* [10], if the Hamiltonian of a composite system can be written as $\hat{H} = \hat{H}_S + \hat{H}_E + \hat{H}_I$ where $\hat{H}_S$, $\hat{H}_E$, and $\hat{H}_I$ correspond to the system, environment, and interaction Hamiltonians, respectively, then weak coupling is characterized by the condition that the interaction energy is much smaller than the typical energies of the subsystems $\sqrt{\langle \hat{H}_I^2 \rangle} \ll \langle \hat{H}_S \rangle, \langle \hat{H}_E \rangle$. This allows the total density matrix to be approximated as a product state, $\hat{\rho}(t) \approx \hat{\rho}_S \otimes \hat{\rho}_E$, enabling a separation between system and environment via partial trace. This assumption is known as the Born approximation. A further implication of weak coupling is the Markov approximation, which neglects system-environment correlations, assuming that the evolution of the system does not depend on the specific state of the environment. Together, these assumptions lead to the Born–Markov quantum master equations used to describe open quantum systems. The most widely used master equation to predict the state evolution of the system is the Gorini–Kossakowski–Sudarshan–Lindblad or Lindblad equation [11–13], which provides a general framework for Markovian dynamics. However, it is not valid for strongly coupled systems, as it fundamentally relies on the Born–Markov assumptions [12].

These master equations are linear extensions of the Schrödinger equation that include operators describing dissipation and decoherence. They have shown good agreement with experimental data [14–16] and have even served as the foundational model for explaining relaxation processes in qubits [17]. Due to their accuracy in describing the relaxation dynamics of single qubits, these models have been extended to more complex two-level systems [16, 18–20].

An alternative approach to studying quantum decoherence is based on the steepest-entropy-ascent (SEA) principle, which considers decoherence as a result of internal irreversibilities occurring during the state evolution of a single or composite system along a path of maximum entropy production toward a state of stable equilibrium [21–25]. This framework, known as SEA quantum thermodynamics (SEAQT), has been effectively employed to describe non-equilibrium phenomena at various levels of description [26–32]. Within an open quantum system, the SEAQT framework considers that environmental interactions can induce a relaxation process through heat transfer between the system and its surroundings. This heat exchange occurs at a constant environmental temperature, driving the quantum system toward a thermal equilibrium state via spontaneous emission, that is, through a relaxation process [33]. In the absence of environmental interactions, the system undergoes decoherence without dissipation.

In this framework, the coupling between the system and its environment is not limited to weak interactions. In fact, when a composite system is considered, it has been argued that there is no physical reason to expect two identical subsystems, $\rho_A = \rho'_A$, to evolve in the same way if each is initially correlated differently with another system B, such that $\rho_B \neq \rho'_B$. In other words, this equation of motion does not assume Markovian dynamics [25].

Nevertheless, decoherence is not the only phenomenon that can be described by the dynamics of both the Lindblad and SEAQT frameworks; the loss of quantum correlations can also be effectively predicted. In this context, quantum discord serves as a measure of quantum correlations that evolve as the system interacts with its environment, regardless of whether the dynamics are governed by Markovian or non-Markovian approaches [34–36]. Notably, quantum discord does not vanish even when the system reaches a stable equilibrium state, indicating that it extends beyond entanglement by capturing a broader spectrum of quantum correlations [37]. This is achieved by comparing classical and quantum information encoded within a bipartite system, i.e. a system composed of two interacting subsystems. For this reason, it is crucial to employ a model capable of describing the evolution of such a composite system, which, in this case, consists of a qubit and its surrounding environment.

In this work, the relaxation time and state evolution of a transmon qubit induced by interactions with an environment are studied using both the SEA and open-system approaches. This phenomenon was previously investigated experimentally by Wang *et al* [38]. The qubit is initially prepared in a mixed state close to the excited state and relaxes toward the ground state. The environment is modeled as a collection of non-interacting harmonic oscillators. The study of this particular system provides insights into the mechanisms of decoherence and, consequently, offers strategies for preserving entanglement and quantum correlations in quantum computers for longer periods.

The remainder of the paper is organized as follows: section 2 provides a description of the model; section 3 presents the results and discusses the findings; and finally, section 4 concludes the paper.

2. Mathematical model

2.1. SEAQT framework

In the SEAQT framework, the state evolution of a quantum system, $\hat{\rho}$, is governed by two components: a symplectic (unitary) term and a dissipative (non-unitary) term. The unitary, or von Neumann, term captures the reversible (linear) dynamics of state evolution, while the dissipative term accounts for the irreversible (nonlinear) dynamics and ensures that the system evolves in the direction of maximum entropy generation.

The SEAQT equation of motion for an isolated quantum system, i.e. one without work, heat, or mass interactions is given by [39]

$$\frac{\mathrm{d}\hat{\rho}}{\mathrm{d}t} = -\frac{i}{\hbar}\left[\hat{H},\hat{\rho}\right] - \frac{1}{\tau_D}\hat{D} \tag{1}$$

where $\hat{H}$ is the Hamiltonian operator, $\hat{\rho}$ is the density operator, $\hbar$ is the reduced Planck constant, τ_D is the internal relaxation time considered as a positive constant or a positive functional of the density operator, and $\hat{D}$ is the dissipative operator, given by

$$\hat{D} = \frac{1}{2}\left[\sqrt{\hat{\rho}}\tilde{D} + \left(\sqrt{\hat{\rho}}\tilde{D}\right)^{\dagger}\right] \tag{2}$$

where $\tilde{D}$ is given as

$$\tilde{D} = \frac{\begin{vmatrix} \sqrt{\rho}\,\ln\hat{\rho} & \sqrt{\hat{\rho}}\hat{I} & \sqrt{\hat{\rho}}\hat{H} \\ \left(\hat{I},\ln\hat{\rho}\right) & \left(\hat{I},\hat{I}\right) & \left(\hat{I},\hat{H}\right) \\ \left(\hat{H},\ln\hat{\rho}\right) & \left(\hat{H},\hat{I}\right) & \left(\hat{H},\hat{H}\right) \end{vmatrix}}{\begin{vmatrix} \left(\hat{I},\hat{I}\right) & \left(\hat{I},\hat{H}\right) \\ \left(\hat{H},\hat{I}\right) & \left(\hat{H},\hat{H}\right) \end{vmatrix}} \tag{3}$$

where $(\hat{F},\hat{G})$ for any operators F and G on $\mathcal{H}$ is given as

$$\left(\hat{F},\hat{G}\right) = \left(\hat{G},\hat{F}\right) = \frac{1}{2}\mathrm{Tr}\left(|\hat{\rho}|\left\{\hat{F},\hat{G}\right\}\right) \tag{4}$$

and $\{\hat{F},\hat{G}\} = \hat{F}\hat{G} + \hat{G}\hat{F}$, is the anticommutator operator. Equation (3) can also be written in terms of the difference operator $\Delta\hat{F} = \hat{F} - \langle\hat{F}\rangle\hat{I}$, where $\langle\hat{F}\rangle = \mathrm{Tr}(\hat{\rho}\hat{F})$, such as

$$\tilde{D} = \frac{\begin{vmatrix} -\sqrt{\hat{\rho}}\Delta\hat{S} & 0 & \sqrt{\hat{\rho}}\Delta\hat{H} \\ -\langle\hat{S}\rangle & 1 & \langle\hat{H}\rangle \\ -\langle\hat{H}\hat{S}\rangle + \langle\hat{H}\rangle\langle\hat{S}\rangle & 0 & \langle\hat{H}^2\rangle - \langle\hat{H}\rangle^2 \end{vmatrix}}{\langle\hat{H}^2\rangle - \langle\hat{H}\rangle^2} \tag{5}$$

where $\hat{S}$ is the entropy operator,

$$\hat{S} = -k_B\hat{B}\ln\hat{\rho} \tag{6}$$

and $\hat{B}$ is obtained from $\hat{\rho}$ by substituting with unity its nonzero eigenvalues,

$$\hat{B} = \hat{B}^2, \qquad \left[\hat{B},\hat{\rho}\right] = 0, \qquad \hat{B}\hat{\rho} = \hat{\rho} \tag{7}$$

Equation (5) can also be expressed in terms of the covariance, $\langle\Delta\hat{A}\Delta\hat{B}\rangle = \mathrm{Cov}(\hat{A},\hat{B})$, as follows

$$\tilde{D} = -\sqrt{\hat{\rho}}\Delta\hat{S} + \beta\sqrt{\hat{\rho}}\Delta\hat{H} \tag{8}$$

where

$$\beta = \frac{\langle\Delta\hat{H}\Delta\hat{S}\rangle}{\langle(\Delta\hat{H})^2\rangle} \tag{9}$$

and if the free energy operator $\hat{f} = \hat{H} - \theta\hat{S}$ is also introduced; thus, equation (3) is expressed as

$$\tilde{D} = \beta\sqrt{\hat{\rho}}\Delta\hat{f} \tag{10}$$

where $\theta = 1/\beta$ is the thermodynamic temperature, indicating that the dissipative dynamics are driven by fluctuations in the free energy.

Thus, equation (1) can be written as

$$\frac{\mathrm{d}\hat{\rho}}{\mathrm{d}t} = -\frac{i}{\hbar}\left[\hat{H},\hat{\rho}\right] - \frac{\beta}{2\tau_D}\left\{\Delta\hat{f},\hat{\rho}\right\} \tag{11}$$

Notice that $\frac{1}{2}\{\Delta\hat{f},\hat{\rho}\} = \frac{1}{2}\{\hat{f},\hat{\rho}\} - \hat{\rho}\langle\hat{f}\rangle$. Thus, the SEAQT dynamics can be interpreted as the evolution of the density matrix due to a symplectic term, compatible with Schrödinger dynamics, and a dissipative term arising from fluctuations in the free energy. This equation of motion is, in fact, trace-preserving and positive definite at all times, as demonstrated in [27].

At a stable equilibrium state, the symplectic term vanishes, implying that the density matrix becomes a function of the Hamiltonian. Consequently, the anticommutator of the free energy also vanishes, and the density matrix takes the form

$$\hat{\rho}_{\mathrm{eq}} = \frac{\hat{B}\mathrm{e}^{-\beta_{\mathrm{eq}}\hat{H}}\hat{B}}{\mathrm{e}^{-\beta\langle\hat{f}\rangle}} \tag{12}$$

Thus, at a stable equilibrium state, the density matrix corresponds to the Gibbs state, and β represents the equilibrium inverse temperature.

2.2. Open quantum system model

An alternative approach to the one described above to predict the state evolution of a system interacting with its environment is the quantum open-system model. One of the most used master equation is the Lindblad equation, which is given as [40]

$$\frac{\mathrm{d}\hat{\rho}}{\mathrm{d}t} = -\frac{i}{\hbar}\left[\hat{H},\hat{\rho}\right] + \frac{1}{2}\sum_j \gamma_j\left(2\hat{L}_j\hat{\rho}\hat{L}_j^\dagger - \left\{\hat{L}_j^\dagger\hat{L}_j,\hat{\rho}\right\}\right) \tag{13}$$

where, $\hat{H}$ is the Hamiltonian operator, $\hat{\rho}$ is the reduced density operator of the system, γ_j are the spontaneous decay rates or damping rates, and $\hat{L}_j$ are the Lindblad operators which model the weak interactions of the system with the thermal reservoir. Here $\hat{L}_j\hat{\rho}\hat{L}^\dagger$ is the usual jump term, and $\{L_j^\dagger\hat{L}_j,\hat{\rho}\}$ is the non-event term which keeps the trace of $\hat{\rho}$ positive definite at all times.

2.3. Projective measurements

To determine the relaxation time T_1 of a qubit, it is studied the process by which the qubit transitions from its excited state $|1\rangle$ to its ground state $|0\rangle$. This process, known as thermal relaxation, thermalization, or amplitude damping, is a fundamental decoherence mechanism that affects the coherence and, consequently, the performance of quantum systems.

The state of the qubit at any time t is described by its density matrix $\hat{\rho}(t)$. To compute the probability of the qubit being in a particular state, projective measurements associated with the corresponding observable

$$\mathcal{O} = \sum_i \lambda_i\hat{P}_i \tag{14}$$

is employed, where λ_i are the eigenvalues corresponding to the measurable outcomes, and $\hat{P}_i$ are the projection operators onto the eigenstates, satisfying the conditions

$$\hat{P}_i\hat{P}_j = \delta_{ij}\hat{P}_i, \qquad \sum_i \hat{P}_i = \hat{I}, \qquad \hat{P}_i^\dagger = \hat{P}_i \tag{15}$$

For the qubit states, the projectors onto the ground and excited states are $\hat{P}_0 = |0\rangle\langle 0|$ and $\hat{P}_1 = |1\rangle\langle 1|$, respectively. The probabilities of finding the qubit in these states at time t are given by

$$\mathrm{Pr}_{|0\rangle}(t) = \mathrm{Tr}\left[\hat{\rho}(t)\hat{P}_0\right], \quad \mathrm{Pr}_{|1\rangle}(t) = \mathrm{Tr}\left[\hat{\rho}(t)\hat{P}_1\right] \tag{16}$$

In the absence of external perturbations other than thermal relaxation, the excited-state probability $\mathrm{Pr}_{|1\rangle}(t)$ decays exponentially over time due to interactions with the environment, such as

$$\mathrm{Pr}_{|1\rangle}(t) = \mathrm{Pr}_{|1\rangle}(0)\,\mathrm{e}^{-t/T_1} \tag{17}$$

thus, assuming the qubit is initially in the excited state, $\mathrm{Pr}|1\rangle(0) = 1$. Thus, the relaxation time T_1 is the characteristic time at which the probability $\mathrm{Pr}|1\rangle(t)$ has decreased to $1/e$ of its initial value, as given by

$$\mathrm{Pr}_{|1\rangle}(T_1) = \frac{1}{e} \tag{18}$$

This exponential decay illustrates how the probability of finding the qubit in the excited state decreases over time due to thermal relaxation. These probabilities are measured through various experiments and plotted as a function of time, forming a curve that is fitted using exponential regression techniques to extract the decay behavior. This process is exemplified by the decay curve obtained in the work by Wang *et al* [38].

2.4. Quantum discord

Quantum discord is a measure of quantum correlations within a quantum system, capturing not only entanglement but also other types of non-classical correlations [37]. In mixed states, the von Neumann entropy includes contributions from both classical and quantum correlations, with classical correlations often dominating. To quantify these correlations, classical mutual information, based on a set of projective measurements, is considered as a measure of classicality, defined as

$$J(\mathcal{S}:\mathcal{A})_{\{P_j^{\mathcal{A}}\}} = S(\mathcal{S}) - S\left(\mathcal{S}|\left\{P_j^{\mathcal{A}}\right\}\right) \tag{19}$$

where $S(\mathcal{S}) = -\mathrm{Tr}\left(\hat{\rho}_{\mathcal{S}}\ln\hat{\rho}_{\mathcal{S}}\right)$ is the von Neumann entropy of subsystem $\mathcal{S}$, and $S\left(\mathcal{S}|\{P_j^{\mathcal{A}}\}\right)$ is the conditional entropy of $\mathcal{S}$ given a set of projective measurements $\{P_j^{\mathcal{A}}\}$ on subsystem $\mathcal{A}$. The conditional entropy is obtained as

$$S\left(\mathcal{S}|\left\{P_j^{\mathcal{A}}\right\}\right) = \sum_j p_j S\left(\hat{\rho}_{\mathcal{S}|j}\right) \tag{20}$$

where $p_j = \mathrm{Tr}\left(\hat{P}_j^{\mathcal{A}}\hat{\rho}_{\mathcal{A}}\right)$ is the probability of obtaining outcome j upon measurement, and $\hat{\rho}_{\mathcal{S}|j}$ is the post-measurement state of $\mathcal{S}$

$$\hat{\rho}_{\mathcal{S}|j} = \frac{\hat{P}_j^{\mathcal{A}}\hat{\rho}\hat{P}_j^{\mathcal{A}}}{p_j} \tag{21}$$

where the projectors $\hat{P}_j^{\mathcal{A}}$ are rank-one operators representing perfect measurements on $\mathcal{A}$.

The quantum mutual information is given as

$$I(\mathcal{S}:\mathcal{A}) = S(\mathcal{S}) + S(\mathcal{A}) - S(\mathcal{S},\mathcal{A}) \tag{22}$$

where $S(\mathcal{A}) = -\mathrm{Tr}\left(\hat{\rho}_{\mathcal{A}}\ln\hat{\rho}_{\mathcal{A}}\right)$ is the entropy of $\mathcal{A}$, and $S(\mathcal{S},\mathcal{A}) = -\mathrm{Tr}\left(\hat{\rho}\ln\hat{\rho}\right)$ is the entropy of the combined system.

In classical information theory, $J(\mathcal{S}:\mathcal{A})$ and $I(\mathcal{S}:\mathcal{A})$ are equivalent, but they differ in the quantum realm due to quantum correlations beyond classical correlations. The quantum discord $\delta(\mathcal{S}:\mathcal{A})$

$$\delta(\mathcal{S}:\mathcal{A}) = I(\mathcal{S}:\mathcal{A}) - J(\mathcal{S}:\mathcal{A}) \tag{23}$$

quantifies this difference. By substituting the expressions for I and J, the quantum discord becomes

$$\delta(\mathcal{S}:\mathcal{A}) = S(\mathcal{A}) - S(\mathcal{S},\mathcal{A}) + S\left(\mathcal{S}|\left\{P_j^{\mathcal{A}}\right\}\right) \tag{24}$$

which is always non-negative and captures the quantum correlations not accounted for by classical mutual information.

To study the dynamics of quantum discord within the SEAQT framework, the rate of change of the relevant entropies is considered. Thus, the rate of change of the total entropy $S(\mathcal{S},\mathcal{A})$ is obtained such as [41]

$$\frac{\mathrm{d}S(\mathcal{S},\mathcal{A})}{\mathrm{d}t} = -\frac{\beta}{\tau_D}\langle\Delta\hat{f},\Delta\hat{S}\rangle \tag{25}$$

where, $\beta = 1/(\kappa_B T)$ is the inverse temperature, τ_D is a dissipative time constant, and $\langle\Delta\hat{f}\Delta\hat{S}\rangle = \langle\hat{f}\hat{S}\rangle - \langle\hat{f}\rangle\langle\hat{S}\rangle$ denotes the covariance between the non-equilibrium free energy operator $\hat{f} = \hat{H} - \theta\hat{S}$ and the entropy operator $\hat{S}$ of the combined system.

Next, the evolution of the entropy $S(\mathcal{A})$ of the thermal bath is considered. The reduced density matrix of $\mathcal{A}$ evolves according to

$$\frac{\mathrm{d}\hat{\rho}_{\mathcal{A}}}{\mathrm{d}t} = -\frac{i}{\hbar}\left[\hat{H}_{\mathcal{A}},\hat{\rho}_{\mathcal{A}}\right] - \frac{i}{\hbar}\mathrm{Tr}_{\mathcal{S}}\left[\hat{H}_{\mathrm{int}}\hat{\rho}\right] - \frac{\beta}{2\tau_D}\left\{\Delta\hat{f}_{\mathcal{A}},\hat{\rho}_{\mathcal{A}}\right\} \tag{26}$$

where, $\hat{H}_{\mathcal{A}}$ is the Hamiltonian of the thermal bath, $\hat{H}_{\mathrm{int}}$ is the interaction Hamiltonian between $\mathcal{S}$ and $\mathcal{A}$, $\Delta\hat{f}_{\mathcal{A}} = \hat{f}_{\mathcal{A}} - \langle\hat{f}_{\mathcal{A}}\rangle$, with $\hat{f}_{\mathcal{A}} = \hat{H}_{\mathcal{A}} - \theta\hat{S}_{\mathcal{A}}$. The rate of change of the entropy $S(\mathcal{A})$ is then given as

$$\frac{\mathrm{d}S(\mathcal{A})}{\mathrm{d}t} = -\frac{\beta}{\tau_D}\langle\Delta\hat{f}_{\mathcal{A}}\Delta\hat{S}_{\mathcal{A}}\rangle \tag{27}$$

The rate of change of the quantum discord is given as

$$\frac{\mathrm{d}\delta(\mathcal{S}:\mathcal{A})}{\mathrm{d}t} = \frac{\mathrm{d}I(\mathcal{S}:\mathcal{A})}{\mathrm{d}t} - \frac{\mathrm{d}J(\mathcal{S}:\mathcal{A})}{\mathrm{d}t} \tag{28}$$

Substituting the expressions for the rates of change, it is obtained

$$\frac{\mathrm{d}\delta(\mathcal{S}:\mathcal{A})}{\mathrm{d}t} = \frac{\beta}{\tau_D}\left(\langle\Delta\hat{f}\Delta\hat{S}\rangle - \langle\Delta\hat{f}_{\mathcal{A}}\Delta\hat{S}_{\mathcal{A}}\rangle\right) - \frac{\mathrm{d}}{\mathrm{d}t}S\left(\mathcal{S}|\left\{P_j^{\mathcal{A}}\right\}\right) \tag{29}$$

To simplify the time derivative of the conditional entropy $S\left(\mathcal{S}|\{P_j^{\mathcal{A}}\}\right)$, note that for time-independent rank-one projectors $\hat{P}_j^{\mathcal{A}}$, the rate of change of $S\left(\mathcal{S}|\{P_j^{\mathcal{A}}\}\right)$ becomes

$$\frac{\mathrm{d}}{\mathrm{d}t}S\left(\mathcal{S}|\left\{P_j^{\mathcal{A}}\right\}\right) = \frac{\mathrm{d}}{\mathrm{d}t}\left(\sum_j p_j S\left(\hat{\rho}_{\mathcal{S}|j}\right)\right) = \sum_j\left(-\mathrm{Tr}\left(\frac{\mathrm{d}\hat{\rho}^j}{\mathrm{d}t}\ln\hat{\rho}\right) + \frac{\mathrm{d}}{\mathrm{d}t}(p_j\ln p_j)\right) \tag{30}$$

where $\hat{\rho}^j = \hat{P}_A^j\hat{\rho}\hat{P}_A^j$. Notice that, since $\hat{P}_j^{\mathcal{A}}$ are time-independent and the measurement process is instantaneous, the change in the conditional entropy due to the measurement is negligible over the timescale of the evolution of the system. Additionally, if the thermal bath is not significantly affected by the dissipative dynamics (i.e. $\tau_D \gg 1$), the conditional entropy remains approximately constant, thus

$$\frac{\mathrm{d}}{\mathrm{d}t}S\left(\mathcal{S}|\left\{P_j^{\mathcal{A}}\right\}\right) \approx 0 \tag{31}$$

Therefore, the rate of change of the quantum discord simplifies to

$$\frac{\mathrm{d}\delta\left(\mathcal{S}:\mathcal{A}\right)}{\mathrm{d}t}=\frac{\beta}{\tau_D}\left(\langle\Delta\hat{f}\Delta\hat{S}\rangle-\langle\Delta\hat{f}_{\mathcal{A}}\Delta\hat{S}_{\mathcal{A}}\rangle\right) \tag{32}$$

Since the covariance terms $\langle\Delta\hat{f}\Delta\hat{S}\rangle$ and $\langle\Delta\hat{f}_{\mathcal{A}}\Delta\hat{S}_{\mathcal{A}}\rangle$ are positive due to the properties of the operators involved, it follows that

$$\frac{\mathrm{d}\delta\left(\mathcal{S}:\mathcal{A}\right)}{\mathrm{d}t}\leqslant 0 \tag{33}$$

This indicates that quantum discord decreases over time under SEAQT dynamics, reflecting the tendency of the system to lose quantum correlations due to dissipative processes. The reduction in discord is associated with the irreversibility inherent in the evolution of the system toward a partially canonical metastable state. Within the SEAQT framework, the rate of change of quantum discord is governed by the entropy generation of both the system and the thermal bath. The projective measurements related to the conditional entropy are linked to the irreversibility of the system, highlighting the thermodynamic nature of quantum correlations. Additionally, the set of projector operators employed corresponds to the eigenstates of the density matrix operator, such that $|\phi\rangle\in\text{rank}\,\hat{\rho}$. Therefore, the projectors must coincide with $\hat{B}$.

2.5. Case of study

As a case study, a total system C is considered, composed of two subsystems denoted as A and B, representing the qubit and the environment, respectively. The environment is modeled as a thermal bath composed of harmonic oscillators. The initial density operator $\hat{\rho}(0)$, representing the initial state of the total system, is given by

$$\hat{\rho}\left(0\right)=\hat{\rho}_A\left(0\right)\otimes\hat{\rho}_B\left(0\right)+\hat{\xi} \tag{34}$$

where $\hat{\rho}_A=\text{Tr}_B\,\hat{\rho}$ and $\hat{\rho}_B=\text{Tr}_A\,\hat{\rho}$ denote the reduced density operators of the qubit and the bath, respectively. The qubit is defined on a Hilbert space $\mathcal{H}_A=\text{span}\{|0\rangle,|1\rangle\}$. The environment is modeled as a collection of harmonic oscillators, each truncated to its two lowest energy levels, effectively reducing each oscillator to a two-level system. The total Hilbert space of the environment is then given by the tensor product $\mathcal{H}_B=\mathcal{H}_{\text{osc}_1}\otimes\mathcal{H}_{\text{osc}_2}\otimes\cdots\otimes\mathcal{H}_{\text{osc}_i}$, with each $\mathcal{H}_{\text{osc}_i}=\text{span}\{|0\rangle,|1\rangle\}$. As a result, the dimension of the environmental state space and the size of the corresponding density matrix $\hat{\rho}_B$ scale exponentially as 2^N, where N is the number of coupled oscillators. To avoid excessive computational burden, the number of oscillators is kept small, while still allowing the model to capture essential features of system-environment interactions, such as transitions between ground and excited states within the environment.

The operator $\hat{\xi}$ accounts for correlations that may exist between the subsystems at initial time. This assumption implies that the system may have interacted with the environment prior to $t=0$, and that such interaction was later turned off, or that the system was not fully isolated at the time of its preparation [25]. The operator $\hat{\xi}$ vanishes when the system and the environment are initially uncorrelated. In the presence of correlations, $\hat{\xi}$ is a Hermitian random operator with zero diagonal elements. This constraint ensures that $\hat{\xi}$ contributes only to the off-diagonal structure of $\hat{\rho}(0)$, thereby encoding inter-subsystem correlations without affecting the normalization condition $\text{Tr}(\hat{\rho})=1$ or the hermicity of $\hat{\rho}$.

The Hamiltonian operator on $\mathcal{H}$ representing the total energy of the composite system is given as

$$\hat{H}=\hat{H}_A\otimes\hat{I}_B+\hat{I}_A\otimes\hat{H}_B+\hat{H}_{\text{int}} \tag{35}$$

Table 1. Initial conditions for the numerical simulation.

Parameter	Value
ω_A	$-1/2$
ω_i	1
g_i	-1
τ_D	0.198
$\hat{\xi}$	$\hat{\xi} = \hat{\xi}^\dagger$, $\hat{\xi}_{ij} = \mathcal{O}(10^{-5})$

where for a qubit coupled to a collection of harmonic oscillators [4],

$$\hat{H}_A = \frac{1}{2}\omega_A \hat{\sigma}_z, \qquad \hat{H}_B = \sum_i \omega_i \left(\hat{b}_i^\dagger \hat{b}_i + \frac{1}{2}\hat{I}\right) \tag{36}$$

and

$$\hat{H}_{\text{int}} = \hat{\sigma}_z \otimes \sum_i \left(g_i \hat{b}_i^\dagger + g_i^* \hat{b}_i\right) \tag{37}$$

where ω_A is the oscillation frequency of the qubit, $\hat{\sigma}_z$ is the $z-$ component of the Pauli operators, ω_i is the oscillation frequency of each harmonic oscillator, i, that conform the thermal bath, g_i is the coupling factor, and $\hat{b}^\dagger$ and $\hat{b}$ are the creation and annihilation operators, respectively.

The model was solved numerically using custom functions in MATLAB®, employing the `ode45` subroutine. This method is based on an explicit fourth-order Runge-Kutta scheme with a variable internal time step to enhance computational efficiency. The convergence criterion is based on the estimated local error at each step, which must remain below a weighted combination of the absolute and relative tolerances. By default, the solver uses a relative tolerance of 10^{-3} and an absolute tolerance of 10^{-6}, unless otherwise specified [42]. The `ode45` subroutine is used to solve equation (11), which governs the time evolution of the density operator of the composite system. A post-processing analysis was carried out using custom functions to evaluate system observables at each time step. The parameter values used in the present model are listed in table 1.

The correlation operator $\hat{\xi}$ in equation (34) is assumed to be very small. Using small values reflects the assumption that the qubit and the environment are nearly uncorrelated, which is typical in scenarios where the system is prepared independently of its environment.

For the initial conditions, it is assumed that the qubit is in a mixed state very close to the excited state $|1\rangle$, while each oscillator in the environment is in a mixed state very close to the ground state $|0\rangle$. A mixed state must satisfy the conditions $\hat{\rho} \neq \hat{\rho}^2$ and $\text{Tr}(\hat{\rho}^2) < 1$. In the Pauli basis, the density matrix is expressed as $\hat{\rho} = \frac{1}{2}(\hat{I} + v_x\hat{\sigma}_x + v_y\hat{\sigma}_y + v_z\hat{\sigma}_z)$, so the initial conditions must satisfy $\sqrt{v_x^2 + v_y^2 + v_z^2} \approx 1$, which ensures that the state is mixed but nearly pure. This assumption reflects a physical scenario in which the qubit is initially in a higher energy state and the environment is in a lower energy state, enabling energy transfer from the qubit to the thermal bath, and leading to its relaxation.

To study the relaxation time T_1 of the qubit interacting with the environment, it is initially assumed that the thermal bath consists of a single harmonic oscillator. Subsequently, the bath is progressively expanded by adding one harmonic oscillator at a time until a total of six oscillators is reached.

The relaxation times predicted by the SEAQT and Lindblad models are compared with the experimental results reported by Wang *et al* where a relaxation time of $T_1 = 0.503$ ms was

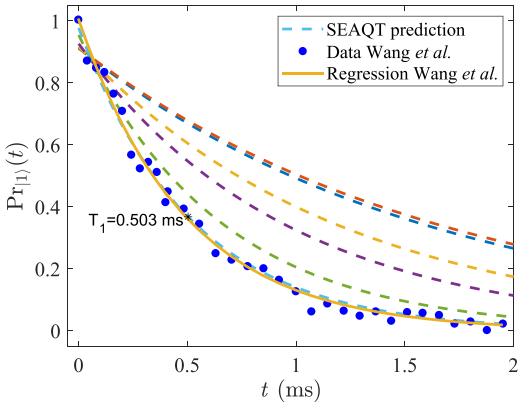

Figure 1. SEAQT prediction of T_1 and a comparison with experimental results reported by Wang *et al* [38]. Each dashed line represents a thermal bath composed with a different number of harmonic oscillators, i.e. $n_{\text{ho}} = 1$-dark blue, $n_{\text{ho}} = 2$-orange, $n_{\text{ho}} = 3$-yellow, $n_{\text{ho}} = 4$-purple, $n_{\text{ho}} = 5$-green, and $n_{\text{ho}} = 6$-light blue. Reproduced from [38]. CC BY 4.0.

measured for a transmon qubit fabricated using tantalum thin films [38]. While transmons constructed from aluminum and niobium are the most widely used, due to their stable superconducting properties and well-established fabrication techniques, the exploration of alternative materials offering improved performance remains an active area of research. It is important to note that the material used to fabricate the qubit does not fundamentally alter the qualitative shape of the relaxation curve, which typically exhibits exponential decay [43–47]. Instead, the material primarily affects the characteristic relaxation time T_1. This observation allows both the SEAQT and Lindblad models to be adapted to match the behavior of different types of qubits, thereby demonstrating their general applicability in the study of relaxation phenomena in superconducting quantum systems.

3. Results and discussion

3.1. SEAQT formulation

Figure 1 shows a comparison between the predicted relaxation time T_1 of the qubit and the experimental data reported by Wang *et al* [38]. It is observed that when the thermal bath is modeled as a collection of six oscillators, the model accurately reproduces the experimental results, yielding a relaxation time of $T_1 = 0.503\,\text{ms}$. This close agreement with the experimental data indicates that the model effectively captures the relaxation dynamics of the qubit.

Figure 2 depicts the expectation value of the energy for the qubit, the thermal bath, and the composite system. As the qubit interacts with the environment, it undergoes a transition from a higher to a lower energy level. The energy released by the qubit is transferred to the thermal bath, resulting in a gradual increase in its energy over time. The figure also shows that the total energy of the composite system remains constant, as expected for an isolated system.

Figure 3 shows the expectation value of the entropy for the qubit, the thermal bath, and the composite system. It can be observed that the entropy increases over time in all three cases.

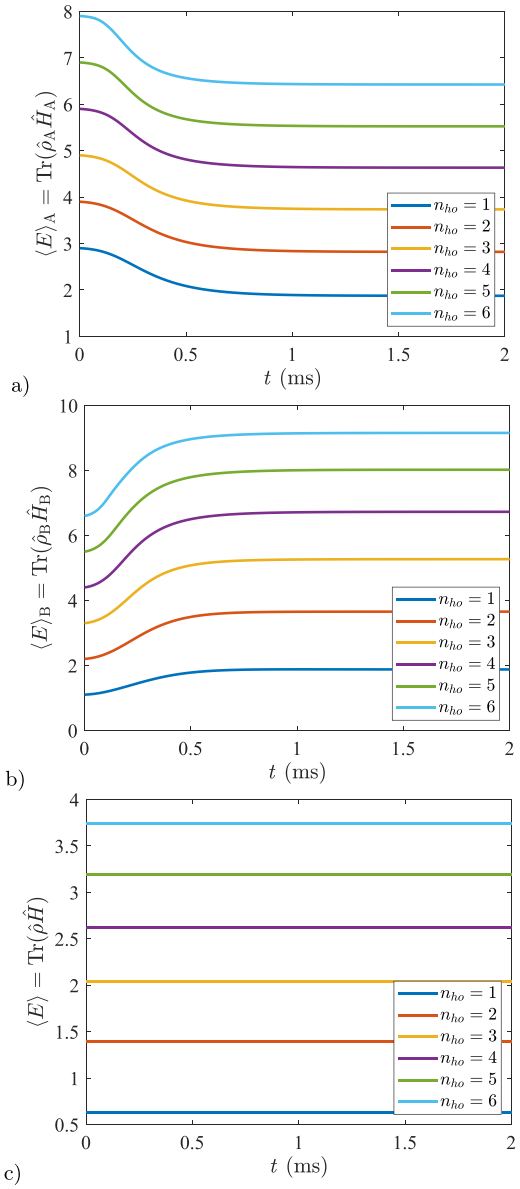

Figure 2. Evolution of the expectation value of the energy for: (a) the qubit, (b) the thermal bath, and (c) the composite system. Each color line represents a thermal bath composed with a different number of harmonic oscillators.

Figure 4 shows the state evolution of the qubit in the form of a Bloch vector. Several scenarios are shown corresponding to a different number of harmonic oscillators for the thermal bath. It is observed that the slowest relaxation occurs when the qubit is interacting with one harmonic oscillator, while the fastest relaxation is observed when the qubit interacts with six harmonic oscillators. Decoherence is observed as the decay of the x and y components of the polarization vector. This decay represents the loss of phase coherence in the state of the qubit

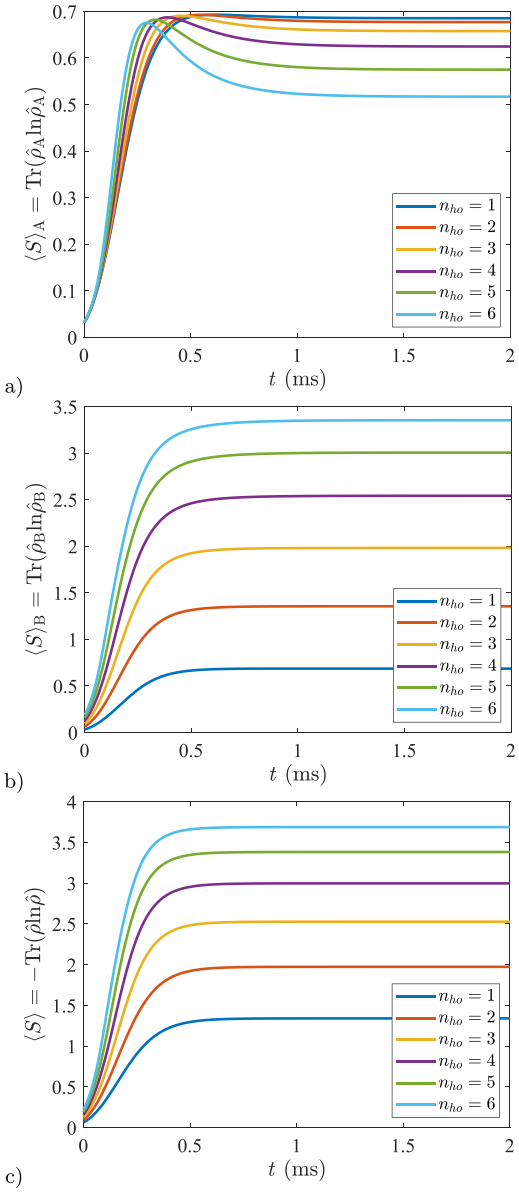

Figure 3. Evolution of the expectation value of the entropy for: (a) the qubit, (b) the thermal bath, and (c) the composite system. Each color line represents a thermal bath composed with a different number of harmonic oscillators.

due to interactions with the environment. In addition, the z component transitions from its initial value towards its equilibrium value, reflecting the energy relaxation of the qubit from the excited state $|1\rangle$ to the ground state $|0\rangle$. The relaxation of the z component corresponds to the T_1 process, while the decay of the x and y components correspond to the T_2 process.

Figure 5 illustrates the qubit dynamics on the Bloch sphere. The qubit is initially prepared in a mixed state near the $|1\rangle$ state, represented by a green point located close to the south pole

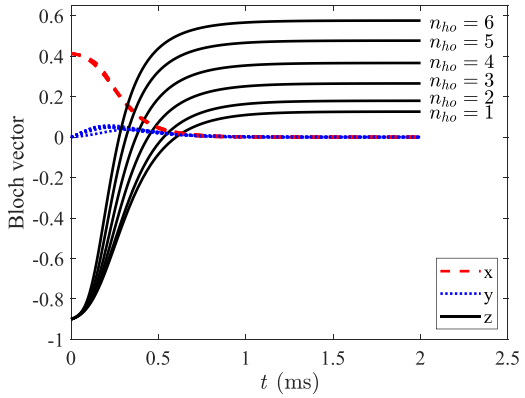

Figure 4. Qubit time evolution of the Bloch vector for the SEAQT formulation.

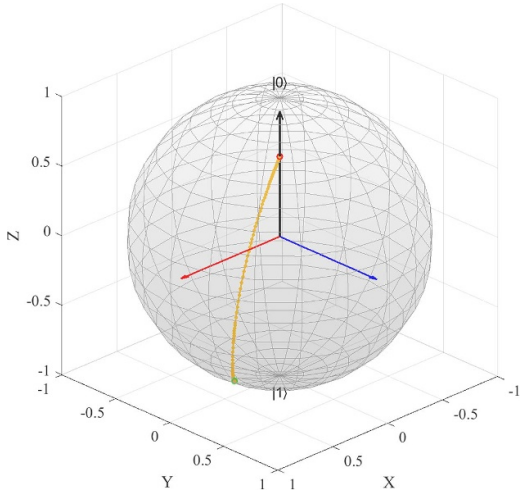

Figure 5. Qubit evolution in the Bloch sphere. The initial condition was chosen with $v_x = \sqrt{0.99^2 - v_z^2},\ v_y = 0,\ v_z = -0.9,$ where $\sqrt{v_x^2 + v_y^2 + v_z^2} \approx 1.$

of the sphere. The final state is indicated by a red point close to the $|0\rangle$ state. As the dynamics induce decoherence, the trajectory evolves inward toward the center of the sphere, reflecting the generation of entropy and the loss of coherence. The system eventually reaches a stable state aligned along the z-axis, where entropy production is maximized and coherence is fully lost.

Figure 6 shows the time evolution of the quantum discord between the qubit and the environment. It is observed that the quantum discord does not decay to zero, even after the qubit has reached its equilibrium state. This non-zero discord arises from the ongoing interactions between the qubit and the thermal bath, indicating that they continue to share quantum information and maintain subtle correlations induced by their interaction.

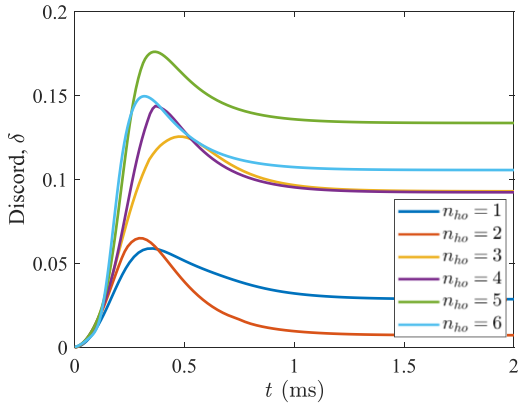

Figure 6. Time evolution of the quantum discord. Each color line represents a thermal bath composed with a different number of harmonic oscillators.

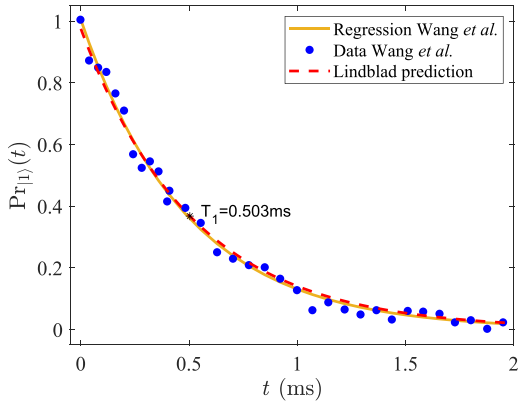

Figure 7. Lindblad prediction of T_1 and a comparison with the experimental results reported by Wang *et al* [38]. Reproduced from [38]. CC BY 4.0.

3.2. Lindblad formulation

The results obtained using the SEAQT framework are compared with those obtained from the Lindblad equation. Figure 7 presents a comparison of the relaxation times T_1 obtained with the Lindblad equation, along with experimental data reported by Wang *et al* [38]. It is observed that the Lindblad equation also provides an accurate prediction of the experimental results. However, data on the state evolution of the thermal bath is not available in this approach, as the Lindblad equation models only the reduced density matrix of the qubit.

Figure 8 shows the time evolution of the qubit obtained with the Lindblad formulation. It is observed that the qubit undergoes a transition from a higher energy state to a lower energy state, a behavior also reflected in the evolution of the Bloch vector. Additionally, the entropy of the qubit initially increases, reaching a peak, and then gradually decreases. Compared to the SEAQT model, decoherence occurs more slowly in the Lindblad model.

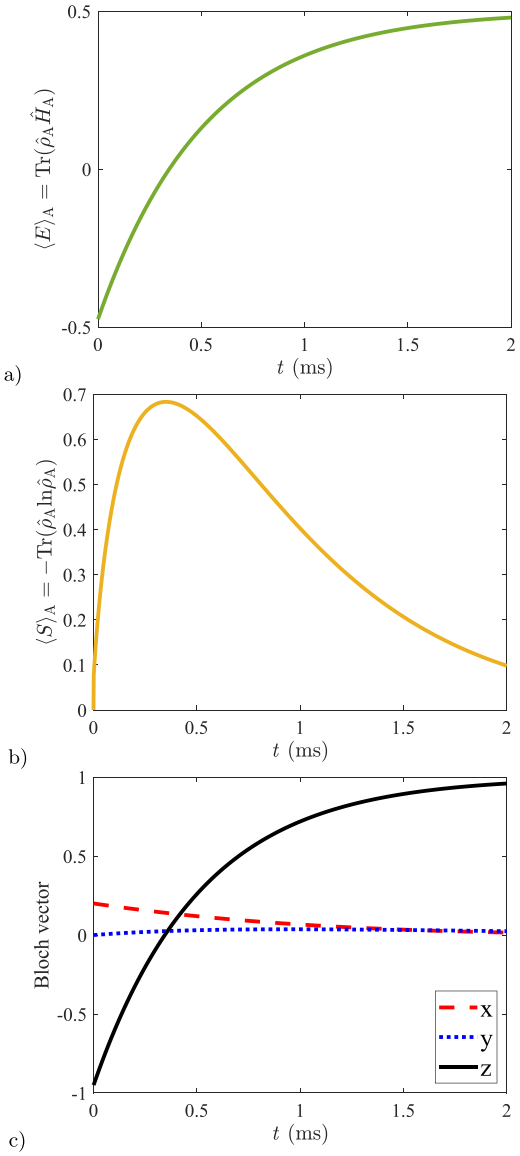

Figure 8. Qubit's time evolution obtained with the Lindblad formulation of: (a) expectation value of the energy, (b) expectation value of the entropy, and (c) Bloch vector.

4. Conclusions

In this work, the relaxation time of a transmon qubit was studied using two frameworks, i.e. the Lindblad and SEAQT approaches. The predicted results were compared with experimental data reported in the literature. Both frameworks accurately reproduce the experimental relaxation time of $T_1 = 0.503\,\mathrm{ms}$. In the SEAQT approach, this result is achieved when the environment (or thermal bath) is modeled as a collection of six harmonic oscillators. A smaller number of oscillators coupled to the system leads to longer coherence times, indicating that

the system is more effectively isolated from its environment. Furthermore, the initial value of the correlation operator $\hat{\xi}$ influences the dynamics of the system, emphasizing that pre-existing correlations with the environment can significantly impact the qubit's relaxation behavior.

Quantum discord is also calculated for the phenomenon under study, providing a broader perspective on quantum correlations beyond traditional entanglement. Even as the qubit reaches a stable equilibrium state, the quantum discord does not vanish completely. This indicates that correlations between the qubit and the thermal bath continue to emerge and dissipate due to the interaction term, although these correlations do not necessarily manifest as entanglement.

In contrast, the Lindblad model does not account for interactions that may have occurred prior to the start of the simulation, as it relies on the Markov approximation, which assumes that such correlations are negligible. Moreover, the model does not require detailed knowledge of the environment's structure, but rather of its overall effect on the system. Therefore, if this effect is accurately captured by the chosen jump operators, the only remaining adjustable parameter needed to reproduce the observed dynamics is the decay rate γ_j. Since the environment is not explicitly modeled in this framework, it is not possible to compute quantum discord, as its evaluation requires knowledge of the entropy of both the system and its environment.

The ability to model both relaxation and decoherence may lead to the development of more efficient error-correction protocols, thereby enhancing the stability and performance of quantum computers.

Future extensions of this work include expanding the model to incorporate additional harmonic oscillators, as well as multiple qubits, enabling the analysis of their performance as a multiprocessor unit. In addition, the implementation of error-correction protocols can be considered to enhance the robustness and accuracy of the system.

Data availability statement

The data cannot be made publicly available upon publication because no suitable repository exists for hosting data in this field of study. The data that support the findings of this study are available upon reasonable request from the authors.

Acknowledgments

L E Rocha-Soto acknowledges the financial support of the Secretariat of Science, Humanities, Technology and Innovation (SECIHTI), Mexico, under its national scholarship program with Grant No. CVU-1146619. C E Damian-Ascencio, S Cano-Andrade, and A Saldaña-Robles gratefully acknowledge the financial support of the University of Guanajuato under Grant No. CIIC 009/2024, and the SECIHTI under its SNII program.

ORCID iDs

Luis Enrique Rocha-Soto 0009-0003-1512-4129
Cesar Eduardo Damian-Ascencio 0000-0003-4515-6570
Sergio Cano-Andrade 0000-0002-1064-7022

References

[1] Klimov P V *et al* 2018 Fluctuations of energy-relaxation times in superconducting qubits *Phys. Rev. Lett.* **121** 090502
[2] Yan F *et al* 2016 The flux qubit revisited to enhance coherence and reproducibility *Nat. Commun.* **7** 12964
[3] Carroll M, Rosenblatt S, Jurcevic P, Lauer I and Kandala A 2022 Dynamics of superconducting qubit relaxation times *npj Quantum Inf.* **8** 132
[4] Schlosshauer M 2019 Quantum decoherence *Phys. Rep.* **831** 1–57
[5] Siddiqi I 2021 Engineering high-coherence superconducting qubits *Nat. Rev. Mater.* **6** 875–91
[6] Lu Y *et al* 2021 Characterizing decoherence rates of a superconducting qubit by direct microwave scattering *npj Quantum Inf.* **7** 35
[7] Brandt H E 1999 Qubit devices and the issue of quantum decoherence *Prog. Quantum Electron.* **22** 257–370
[8] De Leon N P, Itoh K M, Kim D, Mehta K K, Northup T E, Paik H, Palmer B S, Samarth N, Sangtawesin S and Steuerman D W 2021 Materials challenges and opportunities for quantum computing hardware *Science* **372** eabb2823
[9] Proctor T, Rudinger K, Young K, Nielsen E and Blume-Kohout R 2022 Measuring the capabilities of quantum computers *Nat. Phys.* **18** 75–79
[10] Gemmer J, Michel M and Mahler G 2009 *Quantum Thermodynamics: Emergence of Thermodynamic Behavior Within Composite Quantum Systems* vol 784 (Springer)
[11] Lindblad G 1976 On the generators of quantum dynamical semigroups *Commun. Math. Phys.* **48** 119–30
[12] Nakatani M and Ogawa T 2010 Quantum master equations for composite systems: is born–markov approximation really valid? *J. Phys. Soc. Japan* **79** 084401
[13] Chou C H, Yu T and Hu B L 2008 Exact master equation and quantum decoherence of two coupled harmonic oscillators in a general environment *Phys. Rev. E* **77** 011112
[14] Zhang J *et al* 2025 Observation of quantum strong Mpemba effect *Nat. Commun.* **16** 301
[15] Shapira S A, Shapira Y, Markov J, Teza G, Akerman N, Raz O and Ozeri R 2024 Inverse Mpemba effect demonstrated on a single trapped ion qubit *Phys. Rev. Lett.* **133** 010403
[16] Samach G O *et al* 2022 Lindblad tomography of a superconducting quantum processor *Phys. Rev. Appl.* **18** 064056
[17] Nielsen M A and Chuang I L 2010 *Quantum Computation and Quantum Information* (Cambridge University Press)
[18] Dubi Y and Di Ventra M 2009 Relaxation times in an open interacting two-qubit system *Phys. Rev. A* **79** 012328
[19] Žnidarič M 2015 Relaxation times of dissipative many-body quantum systems *Phys. Rev. E* **92** 042143
[20] Shishkov V Y, Andrianov E S, Pukhov A A, Vinogradov A P and Lisyansky A A 2019 Relaxation of interacting open quantum systems *Phys. Usp.* **62** 510
[21] Beretta G P 2010 Maximum entropy production rate in quantum thermodynamics *J. Phys.: Conf. Ser.* **237** 012004
[22] Beretta G P 2006 Nonlinear model dynamics for closed-system, constrained, maximal-entropy-generation relaxation by energy redistribution *Phys. Rev. E* **73** 026113
[23] Beretta G P 2014 Steepest entropy ascent model for far-nonequilibrium thermodynamics: unified implementation of the maximum entropy production principle *Phys. Rev. E* **90** 042113
[24] Montefusco A, Consonni F and Beretta G P 2015 Essential equivalence of the general equation for the nonequilibrium reversible-irreversible coupling (generic) and steepest-entropy-ascent models of dissipation for nonequilibrium thermodynamics *Phys. Rev. E* **91** 042138
[25] Beretta G P 2009 Nonlinear quantum evolution equations to model irreversible adiabatic relaxation with maximal entropy production and other nonunitary processes *Rep. Math. Phys.* **64** 139–68
[26] Cano-Andrade S, Beretta G P and von Spakovsky M R 2015 Steepest-entropy-ascent quantum thermodynamic modeling of decoherence in two different microscopic composite systems *Phys. Rev. A* **91** 013848
[27] Montañez-Barrera J A, von Spakovsky M R, Damian-Ascencio C E and Cano-Andrade S 2022 Decoherence predictions in a superconducting quantum processor using the steepest-entropy-ascent quantum thermodynamics framework *Phys. Rev. A* **106** 032426

[28] Montanez-Barrera J, Damian-Ascencio C E, von Spakovsky M R and Cano-Andrade S 2020 Loss-of-entanglement prediction of a controlled-phase gate in the framework of steepest-entropy-ascent quantum thermodynamics *Phys. Rev. A* **101** 052336
[29] Li G, von Spakovsky M R and Hin C 2018 Steepest entropy ascent quantum thermodynamic model of electron and phonon transport *Phys. Rev. B* **97** 024308
[30] Yamada R, von Spakovsky M R and Reynolds W T 2019 Low-temperature atomistic spin relaxation and non-equilibrium intensive properties using steepest-entropy-ascent quantum-inspired thermodynamics modeling *J. Phys.: Condens. Matter* **31** 505901
[31] Li G and von Spakovsky M R 2018 Steepest-entropy-ascent model of mesoscopic quantum systems far from equilibrium along with generalized thermodynamic definitions of measurement and reservoir *Phys. Rev. E* **98** 042113
[32] Li G and von Spakovsky M R 2016 Steepest-entropy-ascent quantum thermodynamic modeling of the relaxation process of isolated chemically reactive systems using density of states and the concept of hypoequilibrium state *Phys. Rev. E* **93** 012137
[33] Holladay R T 2019 Steepest-entropy-ascent quantum thermodynamic modeling of quantum information and quantum computing systems *PhD Dissertation* Virginia Tech, Blacksburg, VA
[34] Wang B, Xu Z Y, Chen Z Q and Feng M 2010 Non-Markovian effect on the quantum discord *Phys. Rev. A* **81** 014101
[35] Fanchini F F, Werlang T, Brasil C A, Arruda L G E and Caldeira A O 2010 Non-markovian dynamics of quantum discord *Phys. Rev. A* **81** 052107
[36] Werlang T, Souza S, Fanchini F F and Boas C J V 2009 Robustness of quantum discord to sudden death *Phys. Rev. A* **80** 024103
[37] Ollivier H and Zurek W H 2001 Quantum discord: a measure of the quantumness of correlations *Phys. Rev. Lett.* **88** 017901
[38] Wang C *et al* 2022 Towards practical quantum computers: transmon qubit with a lifetime approaching 0.5 milliseconds *npj Quantum Inf.* **8** 3
[39] Beretta G P, Gyftopoulos E P, Park J L and Hatsopoulos G N 1984 Quantum thermodynamics. a new equation of motion for a single constituent of matter *Il Nuovo Cimento B* **82** 169–91
[40] Manzano D 2020 A short introduction to the Lindblad master equation *AIP Adv.* **10** 025106
[41] Damian C, Saldana-Robles A and von Spakovsky M 2024 Non-equilibrium and equilibrium thermodynamic foundations of the 2D toric code within the SEAQT framework (arXiv:2410.24033)
[42] The MathWorks, Inc. 2024 Solve nonstiff differential equations—medium order method MathWorks (Accessed 11 June 2025)
[43] Paik H *et al* 2011 Observation of high coherence in Josephson junction qubits measured in a three-dimensional circuit QED architecture *Phys. Rev. Lett.* **107** 240501
[44] Chang J B *et al* 2013 Improved superconducting qubit coherence using titanium nitride *Appl. Phys. Lett.* **103** 012602
[45] Winkel P, Borisov K, Grünhaupt L, Rieger D, Spiecker M, Valenti F, Ustinov A V, Wernsdorfer W and Pop I M 2020 Implementation of a transmon qubit using superconducting granular aluminum *Phys. Rev. X* **10** 031032
[46] Place A P *et al* 2021 New material platform for superconducting transmon qubits with coherence times exceeding 0.3 milliseconds *Nat. Commun.* **12** 1779
[47] Kim S, Terai H, Yamashita T, Qiu W, Fuse T, Yoshihara F, Ashhab S, Inomata K and Semba K 2021 Enhanced coherence of all-nitride superconducting qubits epitaxially grown on silicon substrate *Commun. Mater.* **2** 98